Taylor & Francis
Taylor & Francis Group

A juvenile specimen of *Anteosaurus magnificus* Watson, 1921 (Therapsida: Dinocephalia) from the South African Karoo, and its implications for understanding dinocephalian ontogeny

Ashley Kruger ⬥ *, Bruce S. Rubidge and Fernando Abdala

Evolutionary Studies Institute and School of Geosciences, University of the Witwatersrand, Johannesburg, WITS 2050, South Africa

Anteosaurid dinocephalians were the apex terrestrial predators of the latter part of the Guadalupian (middle Permian) and became extinct at the end of that epoch. The group was relatively diverse in Russia, but represented by only two genera, *Australosyodon* and *Anteosaurus*, in the Karoo rocks of South Africa. A newly discovered skull of *Anteosaurus magnificus* from the Abrahamskraal Formation is unique among specimens of this taxon in having most of the individual cranial bones disarticulated, permitting accurate delimitation of cranial sutures for the first time. The relatively large orbits and unfused nature of the cranial sutures suggest juvenile status for the specimen. A computer-aided 3D reconstruction of the skull, and comparison with 11 additional individuals, enabled an allometric study of cranial growth in the species. Positive allometry for four of the measurements suggests rapid growth in the temporal region, and a significant difference in the development of the postorbital bar and suborbital bar between juveniles and adults. Pachyostosis was an important process in the cranial ontogeny of *Anteosaurus*, significantly modifying the skull roof of adults. This condition is more obvious in large individuals of the species, but it is recognized that variation may also be independent of growth and could be related to sexual dimorphism. Growth of the skull in *Anteosaurus* shows similar morphological trends to that of the Russian *Titanophoneus* and the Chinese *Sinophoneus*. The overall morphology of the juvenile *Anteosaurus* is clearly reminiscent of the adult skull of the Russian medium-sized *Syodon*, a condition that is more likely a result of similar skull sizes and the lack of strong pachyostosis in adult *Syodon*.

Keywords: Therapsida; Dinocephalia; Anteosauria; *Anteosaurus*; Karoo; Permian

Introduction

Therapsids first appeared in the middle Permian and survive today in the form of mammals. One group of therapsids, the dinocephalians, were particularly abundant during the Guadalupian and went extinct at the end of that epoch (Day *et al*. 2015). Dinocephalians are representative of a stock of large terrestrial tetrapods and have been found in middle Permian rocks of Brazil (Langer 2000; Cisneros *et al*. 2012; Boos *et al*. 2015), China (Li & Cheng 1995; Cheng & Ji 1996; Li *et al*. 1996; Cheng & Li 1997), Kazakhstan (Tchudinov 1968), Russia (Efremov 1954; Orlov 1958; Ivachnenko 1995, 2000), South Africa (Boonstra 1963; Rubidge 1991, 1994; Rubidge & van den Heever 1997; Kemp 2005; Kammerer 2011), Zimbabwe (Lepper *et al*. 2000) and, most recently, Tanzania (Simon *et al*. 2010) and Zambia (Sidor *et al*. 2014).

The rocks of the Beaufort Group of South Africa preserve a vast diversity of Permian to Jurassic tetrapods that have been utilized in the delineation of eight biozones. The *Tapinocephalus* Assemblage Zone has one of the highest diversities of tetrapod taxa of all the Karoo biozones with dinocephalians and dicynodonts, representing 30.7% and 30.9% respectively, of the tetrapod fauna (Smith *et al*. 2011; Day *et al*. 2015). The Dinocephalia includes carnivorous, omnivorous and herbivorous forms, of which the latter are the most abundant in the fossil record (Boonstra 1969; Nicolas & Rubidge 2010). Although they made up a large percentage of the middle Permian terrestrial fauna from the Karoo, dinocephalians became extinct at the end of the *Tapinocephalus* Assemblage Zone towards the end of the Guadalupian epoch (Boonstra 1971; Day 2013; Day *et al*. 2015).

Amongst the carnivorous dinocephalians only *Australosyodon* and *Anteosaurus* are recognized from the South African Karoo (Kammerer 2011). *Australosyodon* was relatively small. By contrast, *Anteosaurus* was a particularly large animal with an adult skull length of ∼800 mm, and was likely a formidable carnivore. The phylogenetic analysis of anteosaurs by Kammerer (2011) recovered a monophyletic Anteosauridae containing two major clades, Syodontinae (including *Australosyodon*, *Notosyodon* and

*Corresponding author. Email: ashleykruger@gmail.com

Syodon) and Anteosaurinae (containing *Anteosaurus*, *Sinophoneus* and *Titanophoneus*). However, the phylogeny of Liu (2013) recovered *Sinophoneus* as a basal anteosaurid outside the Syodontinae-Anteosaurinae split.

A small, almost complete, skull of *Anteosaurus* was recently recovered from the Abrahamskraal Formation (*Tapinocephalus* Assemblage Zone) of the Beaufort Group, South Africa. Here we provide the first detailed description of a complete juvenile *Anteosaurus* skull and discuss morphological changes linked with the ontogeny of the species.

Institutional abbreviations

NHMUK: Natural History Museum, London, UK; **BP**: Evolutionary Studies Institute (formerly Bernard Price Institute for Palaeontological Research) University of the Witwatersrand, Johannesburg, South Africa; **BSPG**: Bayerische Staatssammlung für Paläontologie und historische Geologie, Munich, Germany; **PIN**: Paleontological Institute of the Russian Academy of Sciences, Moscow, Russia; **SAM-PK**: Iziko, South African Museum, Cape Town, South Africa.

Material and methods

The present study is based mainly on a single and almost complete skull, associated with three cervical vertebrae, of a small *Anteosaurus* (BP/1/7074), which was collected in 2011 from mudstone L of the Moordenaars Member of the Abrahamskraal Formation (*Tapinocephalus* Assemblage Zone), Beaufort Group (Jirah & Rubidge 2014). The specimen was discovered on the farm Bullekraal (farm number 251), near Merweville, Beaufort West district, South Africa. Global positioning system (GPS) co-ordinate details are on file at the Evolutionary Studies Institute.

The following anteosaurid cranial material, housed in different South African museums, was also studied for comparative purposes:

BP/1/1369: *Anteosaurus magnificus* – well-preserved specimen consisting of the skull and lower jaws; SAM-PK 11577: *Anteosaurus magnificus* – well-preserved large skull with palate; SAM-PK 4340: *Anteosaurus magnificus* (cotype of *Anteosaurus abeli*) – laterally compressed skull with a complete left lateral side; SAM-PK-K1683: *Anteosaurus magnificus* – skull with a well-preserved left lateral side; SAM-PK 9329: *Anteosaurus magnificus* (holotype of *Anteosaurus acutirostris*) – well-preserved skull with large boss below postorbital bar; SAM-PK 11302: *Anteosaurus magnificus* (holotype of *Anteosaurus crassifrons*) – left lateral side of skull and lower jaw; SAM-PK 11492: *Anteosaurus magnificus* (holotype of *Anteosaurus levops*) – partially prepared skull; SAM -PK-11694: *Anteosaurus*

magnificus (holotype of *Anteosaurus cruentus*) – well-preserved and undistorted skull without the lower jaw; SAM-PK-K284: *Anteosaurus magnificus* – well-preserved specimen with fully prepared skull and palate.

Preparation

Preparation of BP/1/7074 was undertaken by Mrs Cynthia Kemp at the Evolutionary Studies Institute, University of the Witwatersrand. All preparation was mechanical and was undertaken using a Desoutter VP2-X airscribe fitted with tips of tungsten carbide and using paraloid, diluted with acetone, as an adhesive. Because the specimen is a juvenile individual, during the preparation process most of the unfused bones fell apart at their sutures. This resulted in approximately 45 cranial fragments and created a unique opportunity for a detailed description of the specimen. Some of these elements, for example the left prefrontal, frontal, postfrontal, postorbital and squamosal, were fitted and glued back together. Other bones, which were distorted during the fossilization process, could not be fitted in this manner and are curated as isolated elements.

Scanning

BP/1/7074 was scanned using microfocus X-ray computed tomography (CT) with a Nikon Metrology XTH 225/320 LC dual-source industrial CT system. Because of the relatively large size of the specimen, seven individual scans were completed, with each scan incorporating five to 10 elements or fragments. Elements and fragments to be scanned were packed into specially constructed Perspex tubes, which were filled with bubble wrapping. Each scan was completed at 190 KV and 105 µA. Three thousand projections were taken at one frame per second, and a 2.4 mm copper filter was used during the scanning. Scans were reconstructed and segmented using VSG's Avizo® Fire. Two separate scans were stitched together using Volume Graphics' VGStudio Max. Reconstructed scans were exported and segmented as RAW TIFF stacks. Segmentation was completed manually using VSG's Avizo® Fire and Wacom graphics tablets. Once segmentation was completed, elements were exported as PLY (Polygon File Format, also known as the Stanford Triangle Format) files.

Three-dimensional reconstruction of the cranium

As most of the preserved elements of BP/1/7074 have been subjected to some distortion, and the right side of the skull was damaged prior to fossilization, the skull was reconstructed using digital scanning techniques to position each bone in place and build up a full cranial reconstruction. As discussed below, the right side of the skull was generally reconstructed by mirroring parts from the left side.

The right premaxilla, although mostly intact, was removed from the digital reconstruction and mirrored from the left premaxilla. This afforded a more accurate reconstruction of the premaxilla as well as creating a straight connection for the vomers to contact the premaxilla. The nasal was left untouched for the reconstruction, as most of this bone is preserved. The right maxilla, jugal, lacrimal, prefrontal, postfrontal, postorbital and squamosal were reconstructed from the better preserved left side, resulting in an almost complete reconstruction, excluding only part of the lacrimal and jugal, and affording the ability to correct anteroposterior deformation that occurred during the fossilization process

As the occipital bones were all preserved, it was necessary to reconstruct only the right parietal from the left side and fit it to the corresponding tabular and supraoccipital.

In the palate the right vomer was reconstructed from the left one and the two vomers then fitted neatly in an oval groove preserved in the posterior section of the premaxilla. Only the right palatine boss is preserved, so the anterior projection of this bone was mirrored from the left side. The right pterygoid was also mirrored from the left and straightened out to create a more symmetrical depiction of the posterior end of the palate. The basisphenoid is complete and no reconstruction was needed to fit it to the pterygoids anteriorly and the basioccipital posteriorly.

Following reconstruction of the skull, three incisors that had moved from their life position were manually segmented from the 3D scan and accurately repositioned in their respective alveoli in the premaxilla, depicting how they would have been placed in life.

Allometric analysis

Because of the availability of a number of prepared *Anteosaurus* skulls of different sizes in South African museum collections, an allometric analysis was performed using PAST v 2.17C (Hammer *et al.* 2001). The measurement data used in this study were provided by J. A. van den Heever & B. S. Rubidge (pers. comm.). Forty cranial measurements were taken from 15 specimens of *Anteosaurus*. Due to the fragmentary nature of most of the skulls, it was difficult to put together a set of measurements that could be compared in all the specimens. Accordingly, specimens that did not afford sufficient data were removed from the analysis. Thus, a total of 11 specimens and 23 measurements were employed in the final analysis. Measurements were log transformed and analysed using reduced major axis (RMA) regression. In the analysis, b^1 is the slope of the fitted line or coefficient of allometry (Abdala & Giannini 2000).

Measurements of the comparative sample were taken using a sliding Vernier calliper and tape (Fig. 1). To eliminate the effects of distortion during the fossilization process, measurements of BP/1/7074 were taken digitally on
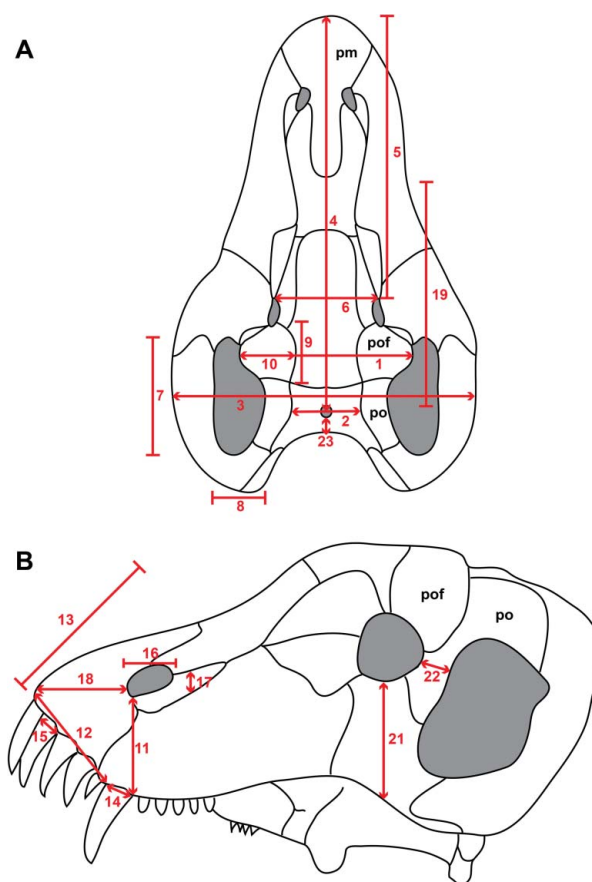

Figure 1. Illustration of the skull of *Anteosaurus* showing the measurements used in the allometric analysis; **A**, dorsal view and **B**, lateral view. Abbreviations: pm, premaxilla; po, postorbital; pof, postfrontal. Redrawn after Boonstra (1969).

the reconstructed skull in Avizo® Fire (Supplemental Data 1). A description of the variables used and the raw measurement data used in the allometric analysis are presented in Supplemental Data 1. Measurements used in the allometric analysis are summarized in Table 1.

Systematic palaeontology

Subclass **Synapsida** Osborn, 1903
Order **Therapsida** Broom, 1905
Infraorder **Dinocephalia** Seeley, 1894
Family **Anteosauridae** Boonstra, 1954a
Subfamily **Anteosaurinae** Boonstra, 1954a
Genus *Anteosaurus magnificus* Watson, 1921
(Figs 2–5)

Holotype. NHMUK R3595, a partial skull.

Age and stratigraphy. Guadalupian (middle Permian) *Tapinocephalus* Assemblage Zone, Abrahamskraal Formation, Beaufort Group.

Table 1. Summary of the regressions on the skull length from the tip of the snout to the middle of parietal (variable 4) of *Anteosaurus magnificus*. Abbreviations: b_1 RMA, coefficient of allometry calculated via reduced major axis method; Iso, isometry; *n,* sample size; Neg, negative allometry; Pos, positive allometry; R^2, adjusted coefficient of determination. There is no correlation (nc) in regression of variables 8 (p 0.20), 9 (p 0.17), 14 (p 0.06), 15 (p 0.81), 17 (p 0.06), 19 (p 0.12), 20 (p 0.26), 23 (p 0.43). Allometric trends are indicated in bold.

Variables	n	R^2	$\log b_0$	b_1	$P_{(ISO)}$	Trend
1. Skull width across postorbital bar	9	0.91	−0.53	1.09	0.481	iso
2. Skull width across parietals over pineal opening	8	0.63	−2.40	1.60	0.183	iso
3. Skull width across squamosals	6	0.81	−0.14	1.01	0.964	iso
5. Skull length of tip of snout to anterior margin of orbit	10	0.96	0.048	0.92	0.265	iso
6. Interorbital distance (anterior margin of orbit)	10	0.53	−1.01	1.15	0.609	iso
7. **Anteroposterior length of temporal fenestra**	8	0.91	−4.34	2.45	**0.003**	**pos**
8. Width of temporal fenestra (parietal-postorbital suture in line with pineal foramen to squamosal bar)	6	0.37	−1.85	1.48	0.463	nc
9. Anteroposterior length of postfrontal	8	0.29	−1.40	1.23	0.609	nc
10. Transverse width of postfrontal	7	0.72	−3.03	1.86	0.107	iso
11. Height from lower margin of external naris to alveolar margin immediately behind canine	9	0.72	−2.45	1.64	0.089	iso
12. Distance anterior margin of canine to tip of snout	10	0.76	−1.40	1.29	0.228	iso
13. **Length anterior margin of premaxilla to posterior extremity of posterior process**	7	0.90	−3.53	2.13	**0.012**	**pos**
14. Anteroposterior length of canine at gumline (largest canine)	9	0.42	−5.32	2.56	0.072	nc
15. Anteroposterior width of the second upper incisor at gum line	6	0.02	−4.11	2.05	0.359	nc
16. Anteroposterior length of naris	8	0.49	−3.10	1.78	0.184	iso
17. Dorsoventral height of naris	7	0.54	−2.85	1.63	0.258	nc
18. Distance anterior margin of premaxilla to anterior margin of external nasal opening	8	0.47	−4.03	2.22	0.114	iso
19. Length between anterior margin of parietal foramen and anterior extent of fronto-nasal boss	10	0.27	−3.02	2.00	0.137	nc
20. Canine width	6	0.30	7.12	−2.18	0.025	nc
21. **Height of jugal below orbit**	9	0.92	−2.37	1.61	**0.009**	**pos**
22. **Width of postorbital bar**	7	0.94	−3.02	1.72	**0.011**	**pos**
23. Posterior margin of pineal foramen to occipital rim	6	0.16	−4.32	2.16	0.306	nc

Diagnosis. *Anteosaurus magnificus* can be distinguished from all anteosaurs other than the two species of *Titanophoneus* on the basis of an angular boss, heavily pachyostosed skull roof including a massive frontal boss, concave alveolar margin of the precanine region, concave dorsal snout profile, posterolateral cant of the posteriormost upper postcanines, and anteroventrally rotated suspensorium. *Anteosaurus* can be distinguished from *Titanophoneus* on the basis of an oval angular boss and the presence of 'brow horns' formed by the massively pachyostosed postfrontals (after Kammerer 2011).

Remarks. The juvenile form of *Anteosaurus* lacks a heavily pachyostosed skull, frontal boss and 'brow horns', and has a shorter snout and suborbital portion of the jugal, and a reduced angulation of the skull roof.

Description

Skull overview
The skull of BP/1/7074 (Figs 2–5) is well preserved on the left side but has missing elements on the right, which were lost prior to fossilization. Only the anterior portion of the left mandible is preserved. In left lateral view it is evident that the orbit is relatively large compared to the temporal opening (Fig. 2).

The adult form of *Anteosaurus* has a skull length of more than 700 mm with a maximum width of 600 mm (J. A. van den Heever & B. S. Rubidge pers. comm.); in contrast specimen BP/1/7074 has a total skull length of 280 mm. As most *Anteosaurus* skulls are distorted by post mortem deformation (Boonstra 1954c), this poses a difficulty in determining the correct skull measurements. When comparing *Anteosaurus* with other Dinocephalia it is apparent that the snout of *Anteosaurus* is high and narrow relative to the orbital region and the skull has a pronounced lateral flare postorbitally (Figs 3, 4). This means that the widest point of an *Anteosaurus* is across the squamosals (Fig. 5), in the temporal region of the skull.

BP/1/7074 exhibits minimal pachyostosis, which is evident only on the postfrontal and postorbital bones. This is in contrast to adult specimens of *Anteosaurus*, which display strong pachyostosis on the postfrontal boss as well as on the frontals.
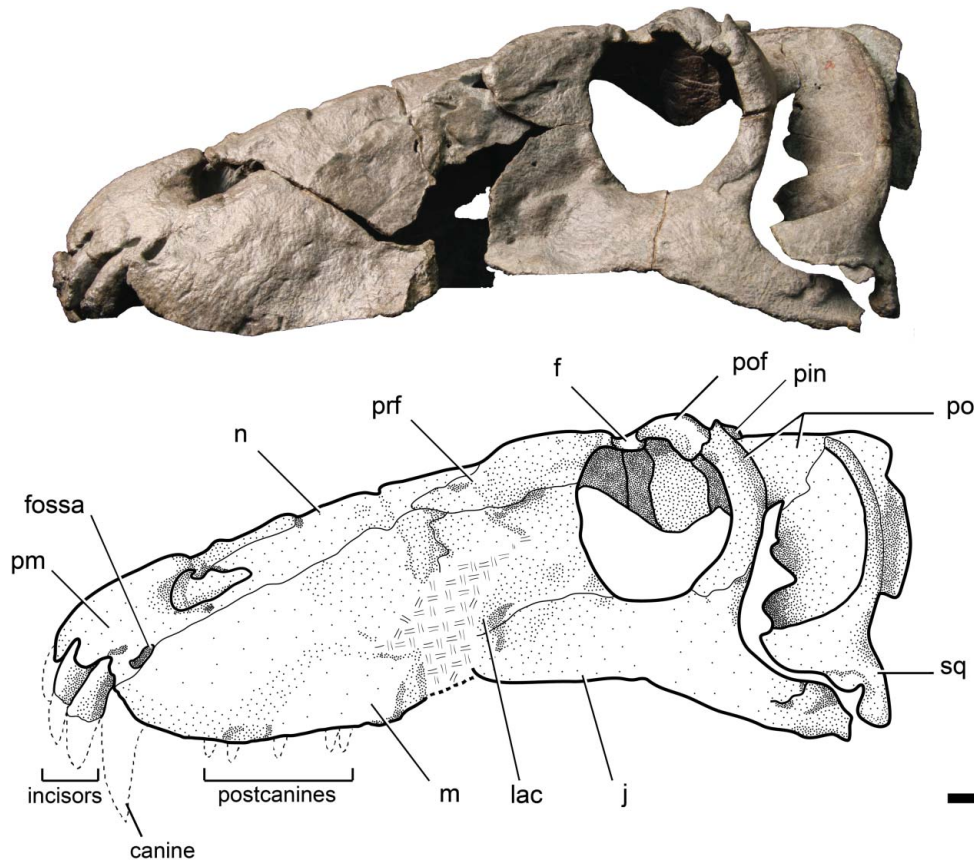
Figure 2. Anteosaurus magnificus Watson, 1921. Photograph and drawing of BP/1/7074 in lateral view. Abbreviations: f, frontal; j, jugal; lac, lacrimal; m, maxilla; n, nasal; pin, pineal foramen; pm, premaxilla; po, postorbital; pof, postfrontal; prf, prefrontal; sq, squamosal. Scale bar = 10 mm.

Skull roof

The premaxilla (Fig. 2) forms the anterior part of the snout and makes up the anterior, dorsal and anteroventral border of the external naris. It extends posterodorsally beyond the posterior border of the external nares. A long antero-posterior sutural contact with the large paired nasals is visible dorsally (Fig. 3), whereas ventrolaterally the premaxilla sutures with the maxilla. In left lateral view a deep fossa is present at the contact with the premaxilla and maxilla, just above and posterior to the last upper incisor. A smaller, shallower fossa is present anteriorly, directly above the last upper incisor. Sutural contact between the premaxilla and maxilla is also visible medially, with a jagged suture that runs down the side of a bulbous canine root within the maxilla (Fig. 4). The left premaxilla slightly overlaps the right premaxilla, showing a posterolateral distortion. Surface texture of the right premaxilla is rougher than that of the left.

There are four upper incisors preserved in the left premaxilla and three in the right. Three incisors fell out of their alveoli prior to fossilization and four incisors are represented only by their roots, still held inside their alveoli.

The septomaxilla is a relatively thin and elongate bone visible on the right side with a short lateral exposure, contacting the premaxilla anteriorly. Posteriorly, it is unclear how far the septomaxilla extends and it appears to end within the margin of the external nares; however, generally *Anteosaurus* is considered to have a large facial exposure of the septomaxilla (Sidor 2003; Kammerer 2011). In another small specimen of *Anteosaurus*, comprising only the snout (SAM-PK-K 4323), the limits of the septomaxilla are not known, and it is believed that the maxilla has a large overlap of the premaxilla (Boonstra 1954a). The nasals are long and narrow, making up much of the dorsal skull roof with a midline nasal suture extending posteriorly, from the premaxilla up to the contact with the frontals (Fig. 3). Anteriorly the nasals contribute to the posterodorsal border of the nares. In left lateral view, the suture between the maxilla and the nasals is very distinct and extends across the lateral side of the skull. The ventral surface of the nasal bones is domed, with two elongate ridges that extend posteriorly towards the prefrontals.

The maxilla is relatively large, covering most of the lateral side of the snout. This bone has a long, dorsal sutural contact with the nasals, and has a pointed posterodorsal
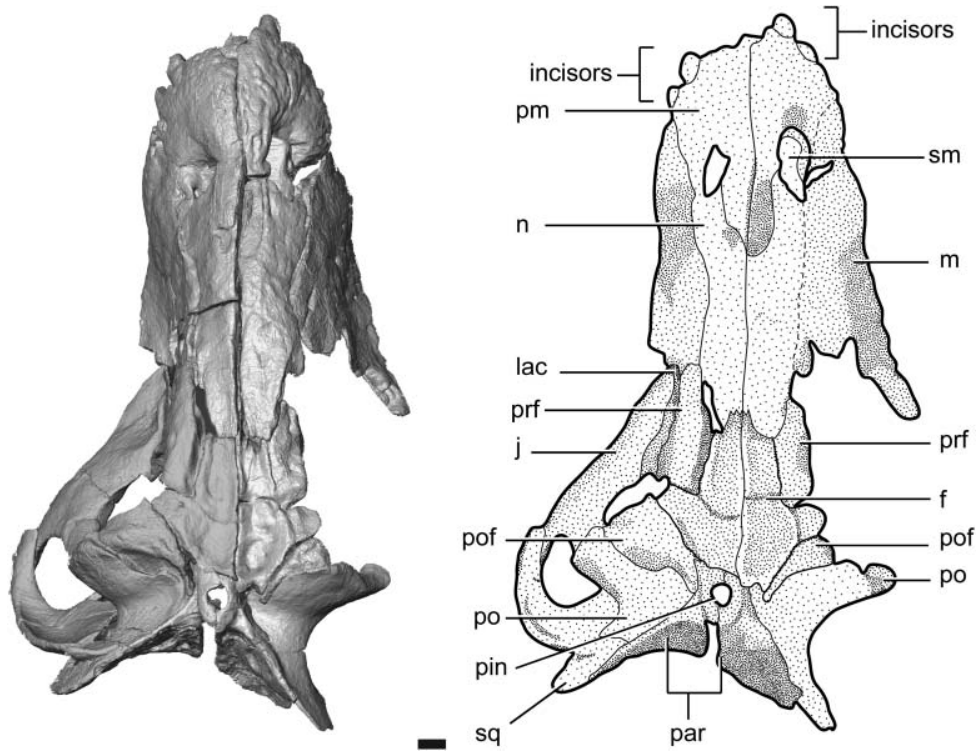
Figure 3. Reconstructed image and drawing of *Anteosaurus magnificus* BP/1/7074 in dorsal view. Abbreviations: f, frontal; j, jugal; lac, lacrimal; m, maxilla; n, nasal; par, parietal; pin, pineal foramen; pm, premaxilla; po, postorbital; pof, postfrontal; prf, prefrontal; sm, septomaxilla; sq; squamosal. Scale bar = 10 mm.
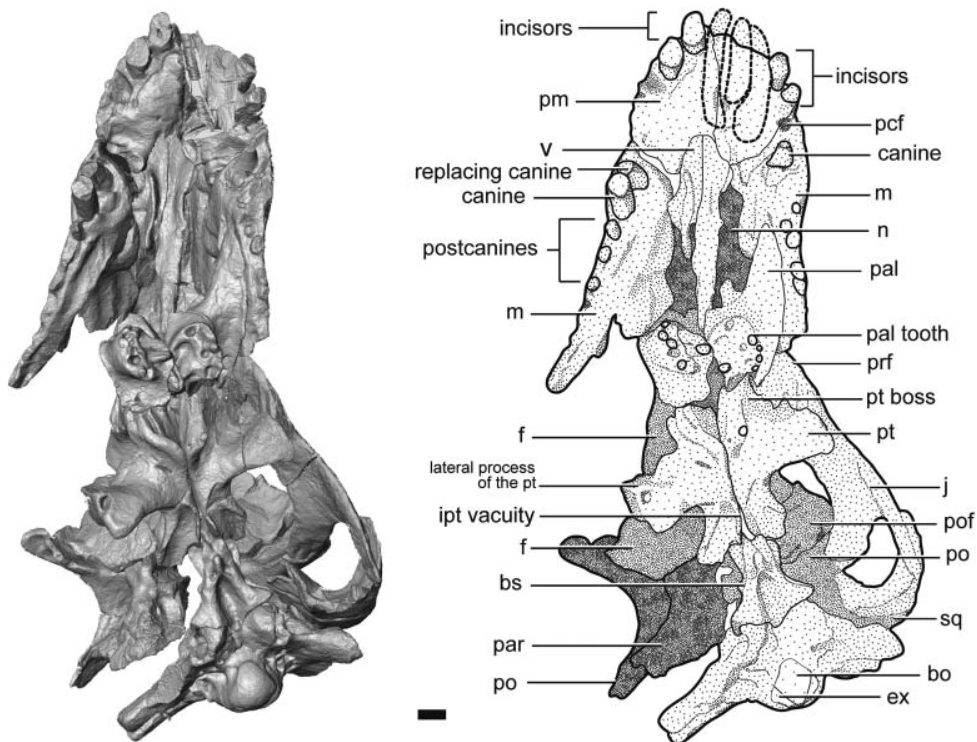

Figure 4. Reconstructed image and drawing of *Anteosaurus magnificus* BP/1/7074 in ventral view. Abbreviations: bo, basioccipital; bs, basisphenoid; ex, exoccipital; f, frontal; ipt, interpterygoid; j, jugal; lac, lacrimal; m, maxilla; n, nasal; pal, palatine; par, parietal; pcf, paracanine fossa; pin, pineal foramen; pm, premaxilla; po, postorbital; pof, postfrontal; prf, prefrontal; pt, pterygoid; sm, septomaxilla; sq, squamosal; v, vomer. Scale bar = 10 mm. Note that three incisors have been segmented out from this reconstruction, but are reflected in the illustration.
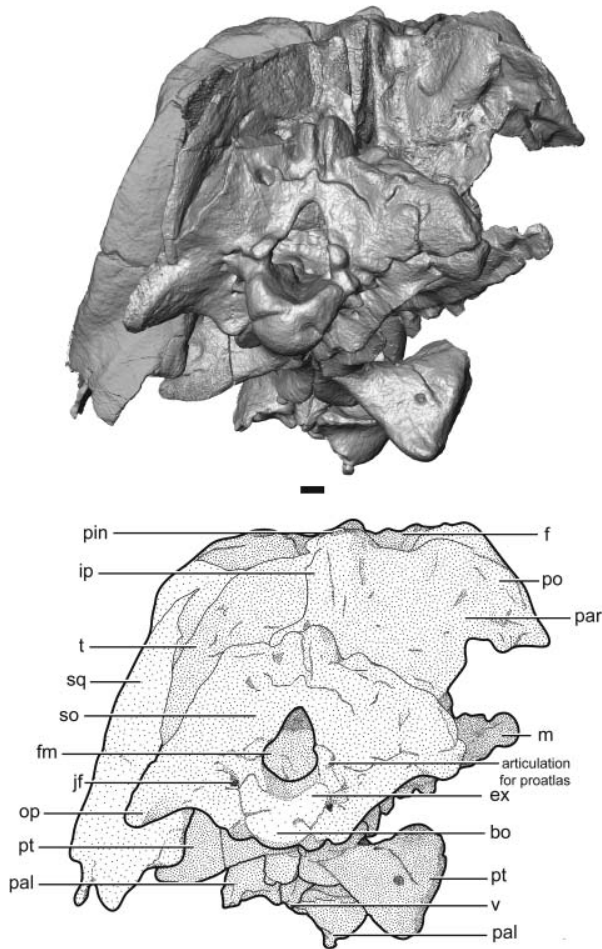
Figure 5. Reconstructed image and drawing of *Anteosaurus magnificus* BP/1/7074 in occipital view. Abbreviations: bo, basioccipital; ex, exoccipital; f, frontal; fm, foramen magnum; ip, interparietal; jf, jugular foramen; m, maxilla; op, opisthotic; pal, palatine; par, parietal; pin, pineal foramen; po, postorbital; pt, pterygoid; so, supraoccipital; sq, squamosal; t, tabular; v, vomer. Scale bar = 10 mm.

contact with the prefrontals. Sutural contact with the anterodorsal portion of the lacrimal is visible on the left lateral side; however, this suture is not preserved ventrally as the specimen is damaged. Boonstra (1954a) stated that the maxilla of *Anteosaurus* has a posterodorsal triangular tongue separating the jugal from the lacrimal. In BP/1/7074 the contact of the maxilla with the jugal is observed medially with a short vertical suture at the ventral margin of the skull, below the orbit. Anterior to the orbit, the maxilla-jugal contact cannot be determined as this part of the skull is not preserved.

In palatal view (Fig. 4) the maxilla creates the posterior border of the paracanine fossa and forms the posterolateral margin of the alveolus of the fifth incisor. On its medial surface, the maxilla typically houses the canine root in a bulbous structure that slopes anteroventrally at

approximately 60 degrees. This housing bulges medially and contains an oval fossa in the middle (Fig. 6). The left boss has a single reasonably well preserved, erupting canine, and on the right side two canines are present. The smaller, anteriorly positioned tooth is the replacement canine. Three postcanine teeth are present on the right maxilla and five are preserved on the left. All the teeth have been damaged and only the bases are preserved. On the posterior edge of the canine housing, and approximately at the mid-level of the bulbous structure, a thin shelf-like ridge extends posteriorly on the medial side of the maxilla to the end of the postcanine row (Fig. 6). The dorsal edge of the ridge leads to a cup-like depression, and the ventral shelf accommodates the antero-ventral projection of the palatine bone. Thus, the maxilla-palatine contact occurs posterior to the canine and anterior to the first postcanine, and continues backward to the posterior margin of the maxilla.

The anterior border of the left lacrimal is damaged, and the right lacrimal is not preserved. Posteriorly the lacrimal of BP/1/7074 forms the anterior border of the orbit, along with the prefrontal. In lateral view, the lacrimal has a horizontally oriented dorsal suture with the prefrontal, which occurs along a small ridge. This suture has a jagged appearance on the medial side of the skull (Fig. 7). The lacrimal meets the jugal with a long horizontal suture. On the medial side of the skull this is a very pronounced and winding suture that extends anteriorly from the inner ventral border of the orbit. The contact between the lacrimal and jugal forms a prominent step, such that the medial surface of the lacrimal overlies that of the jugal.

The jugal is a large bone, forming the ventral border of the orbit (Fig. 2). In lateral view the jugal has its tallest exposure below the posterior orbital margin, where it extends dorsally to contact the postorbital at the base of the postorbital bar. Posterior to the orbit, the jugal forms a small portion of the ventral margin of the temporal fenestra. The outer surface of the jugal, along the ventral border of the temporal fenestra, is overlapped by the zygomatic process of the squamosal.

In lateral view, the prefrontal is an elongate triangular bone with the apex pointing forward between the nasal and maxilla (Fig. 2). Its ventral margin is almost horizontal and forms a clear sutural contact with the lacrimal. The prefrontal forms the anterodorsal part of the orbital border and meets the frontal with a distinctive and depressed suture. Along the dorsal orbital margin, a thick rectangular protrusion of the frontal separates the prefrontal and the postfrontal.

The paired frontals form the skull roof in the orbital region and exhibit a thick protrusion into the dorsal border of the orbit. Thickening of the postorbital bar reduces the contribution of the frontal to the dorsal orbital margin. In ventral view, the frontal is broadly triangular (Fig. 8), with the apex pointing anteriorly.
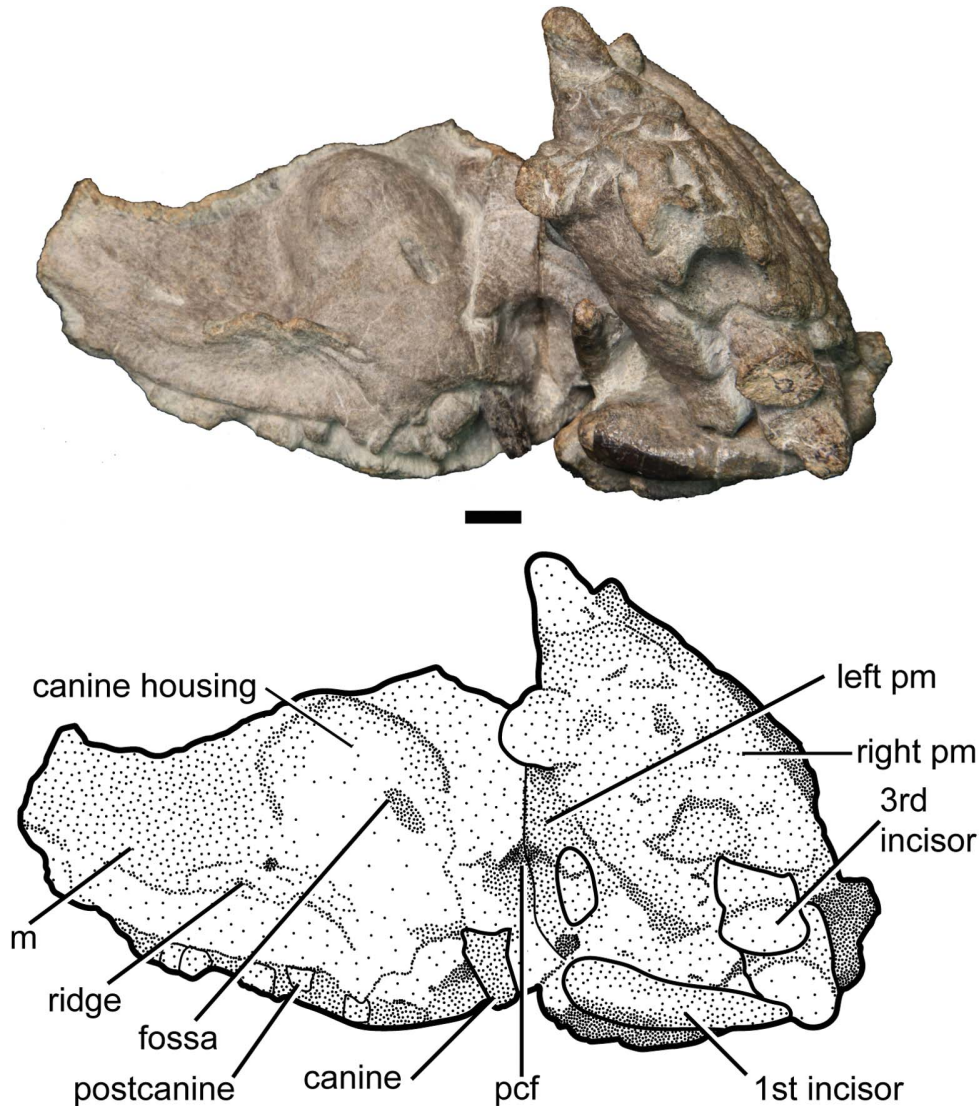
Figure 6. Left maxilla of *Anteosaurus magnificus* BP/1/7074 in medial view. Abbreviations: m, maxilla; pcf, paracanine fossa. Scale bar = 10 mm.

No pachyostosis is evident on the dorsal side of the frontal other than a slight thickening at its contact with the postfrontal. Despite the relatively unpachyostosed appearance of the bone externally, it is clear that the frontals are dorsoventrally thickened. The anterior portion of the frontal is 10 mm thick, whereas the posterior section is 45 mm; however, the skull roof remains flat as the frontal thickens ventrally. At its anterior end, the frontal contacts the nasal along an interdigitated suture. Posteriorly the frontal meets the postfrontal along a ridge that extends obliquely in a posteromedial direction from the dorsal orbital border towards the parietal foramen (Figs 3, 8).

Positioned posterior to the frontal, the postfrontal is a small triangular bone in dorsal view that makes up the posterodorsal orbital border. Its longest side is present along the orbital border and it is thickened to form a boss that overhangs the posterodorsal border of the orbit. From here, the postfrontal tapers to a point between the postorbital laterally and the parietal medially (Figs 3, 8). Posteriorly, the postfrontal has a depression on its dorsal surface anterior to its contact with the postorbital, which has a slight sigmoidal suture and overhang, and this serves as an attachment site for the jaw adductor musculature as has been noted by Kammerer (2011).

The postorbital is roughly triangular, presenting two distinctive surfaces; the lateral surface forms part of the postorbital bar, and the medial surface makes up part of the intertemporal region. The postorbital contacts the jugal to form the postorbital bar. Dorsally, the postorbital
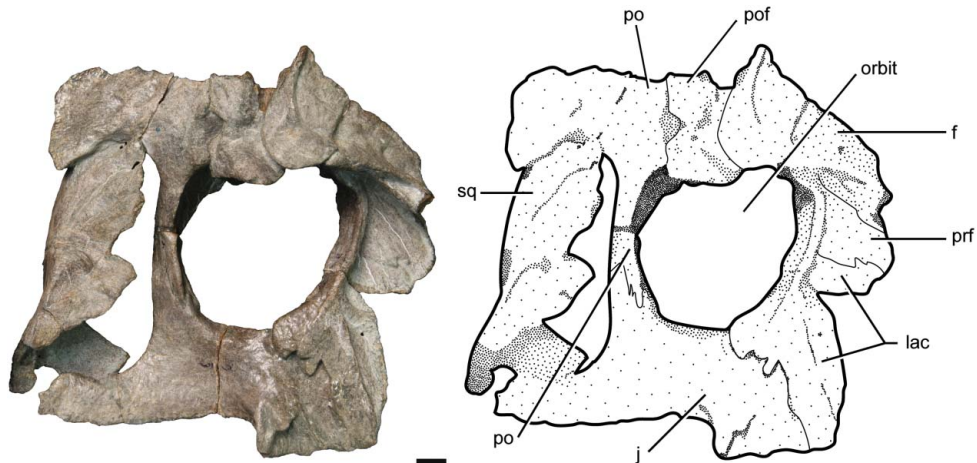
Figure 7. Left medial side of the skull of *Anteosaurus magnificus* BP/1/7074 showing the bones surrounding the orbit. Abbreviations: f, frontal; j, jugal; lac, lacrimal; po, postorbital; pof, postfrontal; prf, prefrontal; sq, squamosal. Scale bar = 10 mm.

is greatly thickened, being thickest at the posterodorsal margin of the orbit. The postorbitals overlap the posterodorsal portion of the postfrontals, forming a trough-like sutural contact between the two bones which is evident in dorsal view (Fig. 3). Dorsomedially the postorbital is a thin sliver of bone forming the lateral face of the intertemporal region. A prominent embayment straddles the contact of the postorbital and postfrontal on the medial aspect of the temporal fossa.

When viewing the bones forming the circumorbital region from the medial side, there is a marked difference in thickness in the different bones. The ventral margin of the orbit, encompassing the jugal and lacrimal, is extremely thin (5 mm) whereas the anterior and posterior margins, being made up of the lacrimal and the postorbital, are considerably thicker (19 mm). The dorsal orbital

border comprising the frontal, postfrontal and postorbital is very thick (38 mm). The thickest part of the orbital border is formed by the postorbital bone, which is not only thicker than any adjacent bones, but is also positioned slightly lower within the orbital border.

The squamosal is a large bone that forms the posterior and ventral borders of the temporal fenestra. It is thinner ventrally but noticeably thickened posteriorly. The left squamosal is well preserved (Fig. 7) whereas the right is missing part of its middle portion. Anterodorsally the squamosal meets the postorbital, whereas dorsomedially it contacts the parietal. The smooth squamosal curves laterally to meet the jugal anteroventrally. Posteromedially, it is covered by the tabular on the occipital surface. Between the zygomatic process and the inner surface of the temporal fenestra is a small notch that housed the quadrate, although the latter element was disarticulated on both sides in BP/1/7074.

Both left and right parietals are preserved, and were separated from the surrounding bones during preparation (Fig. 9). Each parietal is relatively small, quite thick dorsoventrally, and fits neatly behind the curved posterior part of the postorbital on the skull roof. It has an anterior sutural contact with the frontal, which is situated along a transverse ridge, and a small midline anterior projection that extends between the frontals and the medial sides of the postfrontal and postorbital bones. The slightly oval parietal foramen is situated on a large boss at the dorsal end of a long tubular prominence (Fig. 9). In posterior view, a longitudinal median ridge extends from the dorsal edge of the pineal boss to beneath the overlapping interparietal. A posterior view of the parietal bone exposes a short longitudinal sutural contact with the interparietal. At this meeting of the parietal and interparietal, a fossa is present on the right parietal bone, mirrored by a slightly shallower fossa on the left.
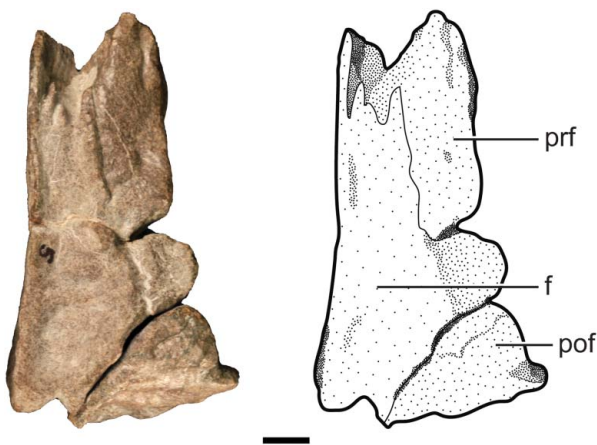

Figure 8. Right prefrontal, frontal and postfrontal of *Anteosaurus magnificus* BP/1/7074 in dorsal view. Abbreviations: f, frontal; pof, postfrontal; prf, prefrontal. Scale bar = 10 mm.
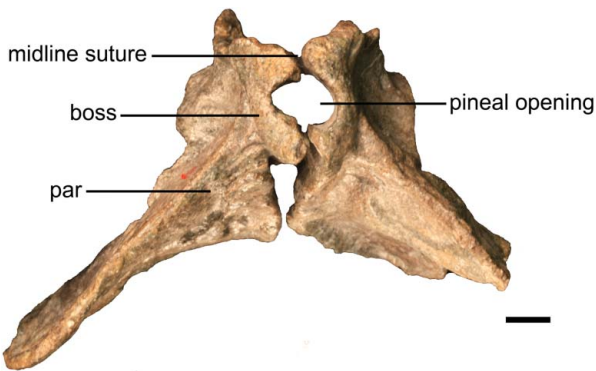
Figure 9. Dorsal view of left and right parietal, and pineal opening of *Anteosaurus magnificus* BP/1/7074. Abbreviation: par, parietal. Scale bar = 10 mm.

Palate

Palatal elements on the left side of BP/1/7074 are generally better preserved than those on the right. The premaxilla is complete but portions of the right vomer and palatine are missing, and the pterygoids and basisphenoid are well preserved. In ventral view (Fig. 4) the premaxilla is relatively small and forms the anterior part of the skull. Posterolaterally it contacts the maxilla with a clear oblique suture anterior to the canine and posterior to the fifth incisor. Posteromedial to the fifth incisor, a paracanine fossa, where the lower canine was housed when the jaws were closed, is present and the suture between the premaxilla and maxilla extends through this fossa. This is different from the suture described for *Australosyodon* (Rubidge 1994) where the maxilla-premaxilla suture is immediately posterior to the paracanine fossa. The maxilla-premaxilla contact in *Anteosaurus* is thus similar to that of *Syodon* and *Titanophoneus* (Orlov 1958) in that all have a suture which transverses the paracanine fossa. Anteromedially the premaxilla creates the anteromedial border of the internal naris.

The paired vomers are complex, elongate bones, with the anterior tip fitting into a midline notch of the premaxilla. In ventral view the vomer has a lateral flange that protrudes ventrally along the entire medial side of the internal nares, and a midline ridge that extends from the anterior end of the vomer to behind the internal nares. On the anterodorsal side, the vomer has a short, rounded lateral protrusion. The vomer continues posteriorly above the enlarged palatine boss as a triangular bulbous structure that is in contact with the dorsal side of the palatine boss (Fig. 10), and is not visible in palatal view.

On the left side, an anterolateral process of the palatine overlies the posteroventral side of the maxilla. Posteriorly the palatine forms a prominent ventrally protruding dentigerous boss. The lateral margins of the palatine bosses each have five small conical teeth arranged in a semicircular row. The palatines meet each other at the midline. Posteriorly the palatine boss meets the pterygoid with a zigzag sutural contact.

The ectopterygoid, which is usually positioned anteromedial to the lateral pterygoid process, is not preserved and probably became disarticulated prior to fossilization.
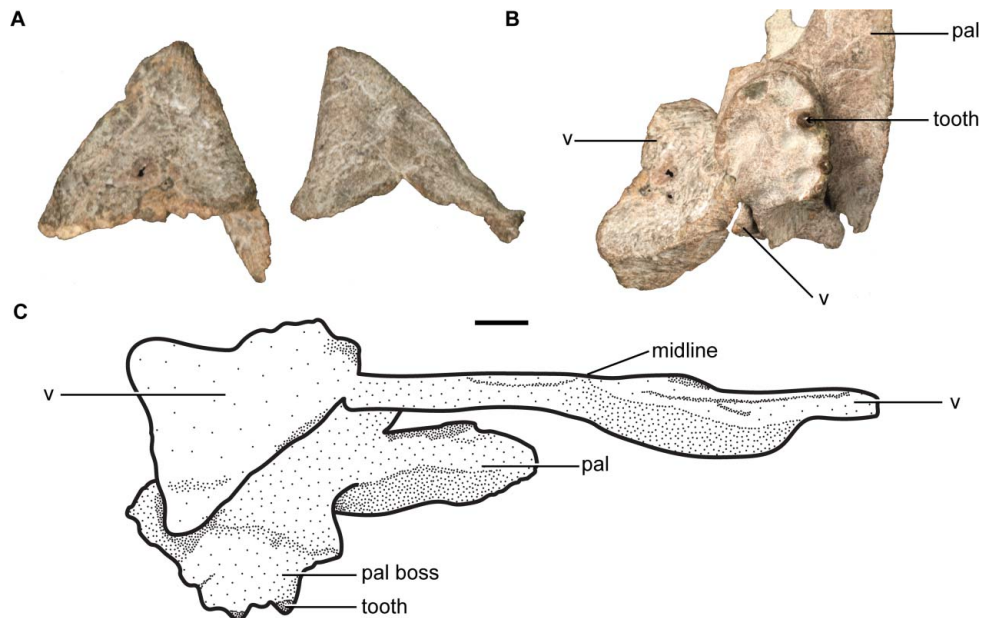

Figure 10. Palate of *Anteosaurus magnificus* BP/1/7074. **A,** posterior projection of the left and right vomer which continues under the palatine in a triangular form, in lateral view; **B,** position of the posterior projection of the vomer with relationship to the palatine and palatine boss; **C,** drawing of a cross section and medial view of the left: vomer, posterior projection of the vomer, and palatine. Abbreviations: pal, palatine; v, vomer. Scale bar = 10 mm.
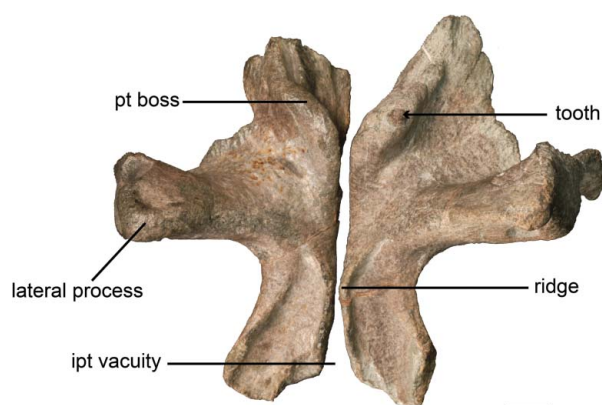
Figure 11. Left and right pterygoids of *Anteosaurus magnificus* BP/1/7074 in ventral view. Abbreviations: ipt, interpterygoid; pt, pterygoid. Scale bar = 10 mm.

Boonstra (1954a) stated that the ectopterygoid met the palatine, maxilla and jugal, forming the upper part of the lateral and anterior face of the lateral pterygoid process. In *Syodon* and *Titanophoneus*, the ectopterygoid contacts the jugal posteriorly, and Boonstra (1954b) believed this to be the situation in *Anteosaurus* as well.

The pterygoid (Fig. 11) is a large bone exhibiting three rami. Anteriorly, the anterior (or palatal) ramus of the pterygoid contacts the palatine boss and anterolaterally has a small contact with the palatine. The anterior ramus has one small conical tooth present on the left side of the palatine boss, but no teeth are visible on the right element. The transverse process of the pterygoid extends laterally, and produces a ridge-like structure that extends to the lateral border of the pterygoid. This is where the pterygoid is thickest and forms a bulge in the middle of the bone. No teeth are evident on the transverse process. The basicranial ramus of the pterygoid curves posteriorly, contacting the basisphenoid. A parasagittal ridge is present on the basicranial ramus of the pterygoid and extends from the transverse processes to the contact with the basisphenoid. A small interpterygoid vacuity is positioned in the midline between the two basicranial rami and the basisphenoid rostrum.

The basisphenoid is a complex bone, possessing many ridges and facets. In ventral view it contacts the basicranial ramus of the pterygoids anteriorly, and widens posteriorly where it meets the basioccipital. Ventrally the basisphenoid has a deep longitudinal trough extending posteriorly from halfway along the corpus to its posterior border. Immediately anterior to this trough, a midline crest is present with a carotid foramen on each side. The midline crest does not extend as far as the anterior margin of the basisphenoid. In lateral view, the dorsal side of the basisphenoid has a prominent rectangular crest. This crest occupies the middle of the corpus, and terminates posteriorly before the interpterygoid vacuity. A posterior view of

the basisphenoid shows a lateral articulation, which meets two corresponding condyles on the basioccipital.

Occiput

The occiput (Fig. 5) is well preserved, missing only a portion of the right tabular, parietal and squamosal. The supraoccipital, opisthotic and tabulars are fused and the foramen magnum is large and triangular.

In occipital view, the unpaired interparietal is best preserved on the left, and a small portion is still apparent on the right side but its borders cannot be delineated with confidence. The parietal extends posteriorly onto the dorsal occipital surface, and the interparietal overlaps it on the posterior side. Ventrally the interparietal has a short contact with the supraoccipital. The interparietal is thin on its dorsal side where it contacts the parietal, and becomes thicker along its ventral border close to the contact with the supraoccipital.

The tabulars are thin, smooth, semilunate curved bones, extending laterally in occipital view and partially covering the posterior portion of the postorbital, parietal and squamosal bones. A larger portion of the left tabular is preserved compared to that of the right. A ridge-like suture is present between the tabular and interparietal.

The supraoccipital is a transversely broad bone, situated ventral to both the interparietal and tabular bones. It forms the dorsal border of the foramen magnum. Posteriorly, the suture between the interparietal and supraoccipital is distinct; however, contact with the tabular is unclear. Ventrally the supraoccipital is completely fused to the opisthotic and it is difficult to make out sutures, even though this specimen likely represents a juvenile.

The opisthotic is a large bone making up the posteroventral part of the occipital region. It forms a concave surface that deepens towards the foramen magnum. The paroccipital process of the opisthotic is more apparent on the right side of the specimen, contacting the supraoccipital dorsally, the basioccipital ventromedially and the tabular dorsolaterally.

Paired exoccipitals, which are triangular and relatively small, form the lateroventral and ventral margin of the foramen magnum. Ventrally they meet the basioccipital, protrude from the ventral and lower lateral margins of the foramen magnum and continue posteriorly onto the occipital condyle. A jugular foramen is present on each side of the occipital condyle, just below the dorsolateral suture of the exoccipitals. Medial to the jugular foramen is a fossa of comparable size. Above the exoccipitals, at the ventrolateral border of the foramen magnum, is a small oval protrusion, which would articulate with the proatlas in life.

In posterior view, the basioccipital is smooth and rounded, wedging between the two posteriorly projecting exoccipitals and creating the ventral portion of the occipital condyle. On the occipital surface, the basioccipital
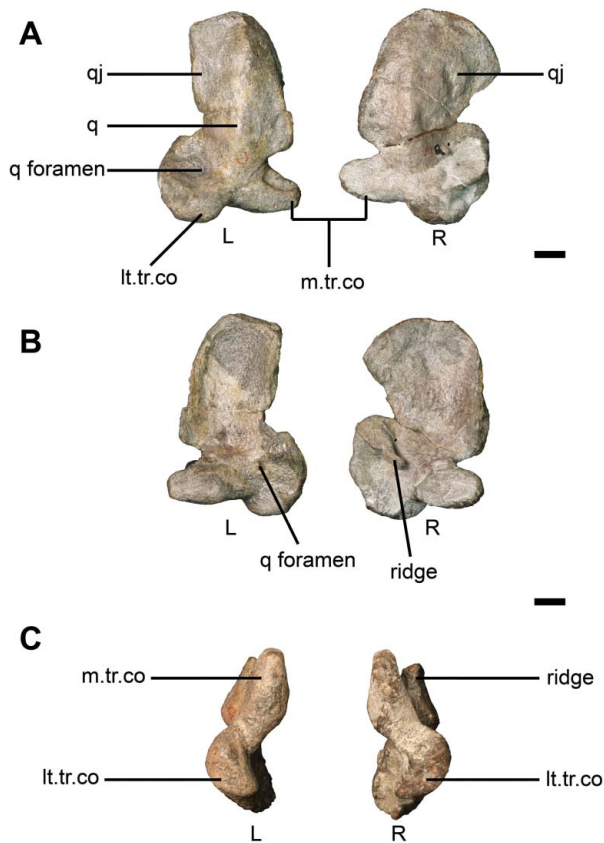
Figure 12. Left and right quadrate bones of *Anteosaurus magnificus* BP/1/7074; **A,** anterior view; **B,** posterior view; **C,** ventral view. Abbreviations: lt.tr.co, lateral trochlear condyle; m.tr.co, medial trochlear condyle; q, quadrate; qj, quadratojugal. Scale bars = 10 mm.

meets the opisthotic dorsolaterally, and on the palate it is in contact with the basisphenoid anteroventrally.

Both quadrates are preserved as isolated elements. Each is a broad spoon-shaped bone and in lateral view has a convex profile (Fig. 12). The dorsal surface of the quadrate is rounded, and in posterior view it has an 'S'-shaped ventral margin formed by two articulatory condyles. The medial trochlear condyle is slightly larger than the lateral trochlear condyle. The contact facet is convex, a small quadrate foramen is present ventrolaterally and a deep lateral notch is also present.

Lower jaw

Only a small anterior portion of the left dentary of BP/1/7074 is preserved (Fig. 13). On the medial side of the left mandible, a broad trough separates the dentary from the splenial. Much of the posterior dentary and splenial is not preserved and thus the nature of this suture is unknown.

Only a very small section of the very weathered angular is preserved, separated from the other elements of the lower jaw.
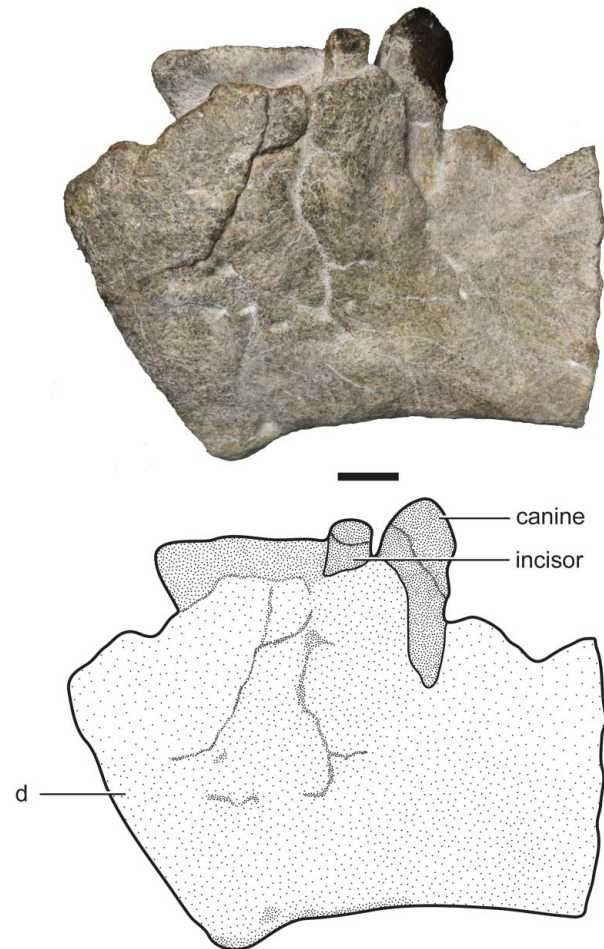

Figure 13. Photograph and drawing of left dentary of *Anteosaurus magnificus* BP/1/7074 in lateral view. Abbreviation: d, dentary. Scale bar = 10 mm.

Dentition

Because three incisors have become dislodged from the alveoli and are lying horizontally across the premaxilla, it is difficult to accurately determine the number of incisor teeth. In our assessment, on the left premaxilla, two large posterior incisors are preserved in their alveoli in front of the paracanine fossa. The three anterior-most alveoli are not visible. On the right side the posterior two alveoli of the premaxilla do not have teeth. The roots of incisors two and three are preserved in their alveoli. Incisor one is dislodged from its alveolus and is lying across the anterior end of the premaxilla. The three anterior incisors (Fig. 14A), which are removed from their alveoli, manifest a simple structure with a pointed root and a more bulbous crown without heels. We consider a single isolated tooth, found lying next to the specimen, to be the fourth right incisor. This well-preserved tooth, which has a slightly posteriorly recurved crown, has a keel on its posterior side, and the anterior medial side is flattened by
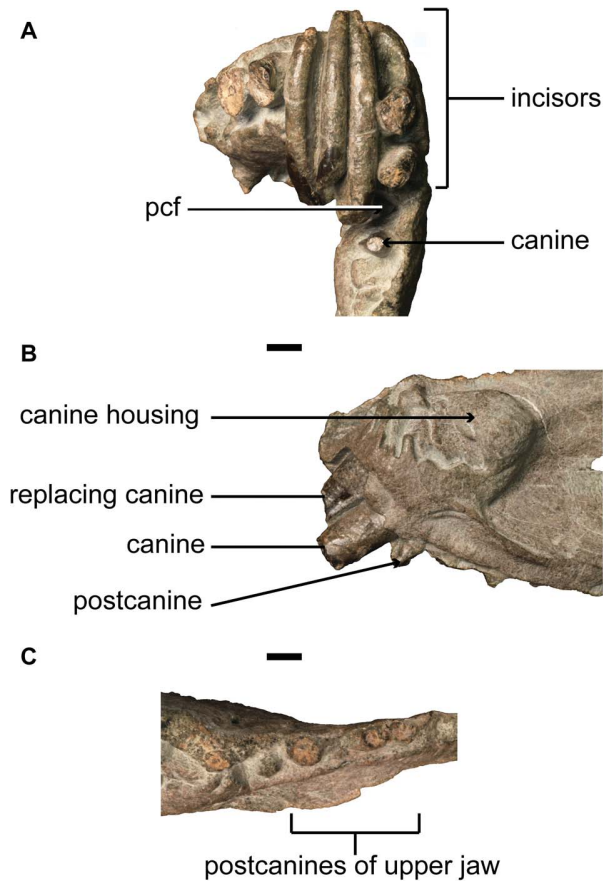
Figure 14. Dentition of *Anteosaurus magnificus* BP/1/7074. **A,** incisors in ventral view; **B,** canine and replacing canine of the right maxilla in medial view; **C,** postcanines of the left maxilla in ventral view. Abbreviation: pcf, paracanine fossa. Scale bars = 10 mm.

occlusal wear from the corresponding incisor of the lower jaw. Broad longitudinal striations are present on the enamel of the crown.

In the left dentary only one incisor and a partial canine are preserved. Only the base of the canine is present, which is oval in cross-section and features longitudinal striations that cover the entire surface. No serrations are present on the lower portion of the canine crown. The canine root is large and causes a bulge on the medial side of the mandible. The preserved incisor is oval in cross section, has a slight posterior curve and does not possess a heel. The incisor is slightly worn and has a wear facet on the anteromedial side, and the crown is damaged.

The left upper canine, which was just erupting at the time of death, is visible with only its crown protruding. On the right side, both the canine and the replacement canine are preserved, and the replacement canine is positioned anterior to the existing canine (Fig. 14B). The upper canine is more robust than the incisors and is longitudinally oval in cross section. The lower canine is

slightly smaller than the upper, but has been broken off just above the alveolus so that most of the crown is not preserved.

The roots of five postcanines are present in position on the left maxilla, and on the right, only three postcanines and an empty posteriorly positioned alveolus are present (Fig. 14C). An even more posteriorly placed flattened portion of the alveoli rim, on the left, might indicate an additional alveolus. The postcanine crowns are all damaged. The roots of the postcanines are oval in cross section and become smaller posteriorly.

In the dentary, no postcanines are preserved but a single alveolus is present posterior to the canine. The canine is preserved in position with half its crown, the tip having been broken off. The base of the last incisor is present in front of the canine, and three alveoli are present anterior to that. The canine is ovoid in cross section with a pointed keel on the posterior margin, and is rounded anteriorly. The lateral surface of the crown is smooth.

A replacing right canine, erupting anteriorly, is clearly visible. CT scanning of the specimen allowed for the observation of replacement incisors and postcanines within the jaws. Only one replacing incisor is present in the left premaxilla (Fig. 15A) and it is deep within the alveolus, suggesting that it is at a very early stage of development. This element seems to be replacing the fourth incisor on the lingual side; however, the locus is not certain. Two very small replacement incisors, located lingual to the functional incisor, are present in the left dentary (Fig. 15B, C). Only a very small replacement postcanine, situated far posteriorly on the left maxilla, is evident (Fig. 15D). Because the new tooth 'bud' is positioned deep in the alveolus, it is unclear whether the replacement tooth is replacing the existing tooth lingually.

Cervical vertebrae

Along with the atlas-axis complex, two post-axial cervical vertebrae were preserved with the skull of BP/1/7074. The atlas centrum and a triangular intercentrum are preserved as loose elements. These elements articulate with each other, making the identification and recognition of these bones as the atlas-axis complex and the following two cervical vertebrae straightforward.

In anterior view, the flat and triangular proatlas attaches with facets on the occipital surface of the skull at the ventrolateral border of the foramen magnum, where an oval protrusion exists just above the exoccipital and basioccipital condyle.

In dorsal view, the atlas centrum has a broad midline trough, which forms the floor of the neural canal (Fig. 16). Dorsolaterally a pair of flat odontoid processes is positioned lateral to the neural canal. Posterior to the odontoid process, the bone slopes posteroventrally to the posterior margin of the atlas centrum.
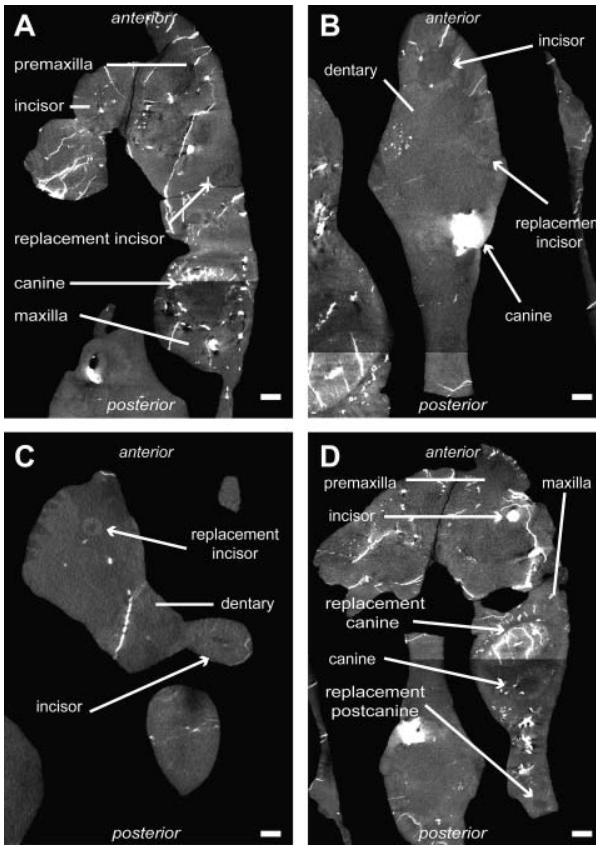
Figure 15. CT slice image. **A,** left premaxilla indicating replacement incisor; **B,** left dentary indicating replacement incisor; **C,** left dentary indicating replacement incisor; **D,** left maxilla indicating replacement canine and postcanine of BP/1/7074. Scale bars = 10 mm.

The axis (Fig. 17) broadly resembles the two post-axial cervical vertebrae in morphology, but the axial neural spine is typically much shorter and broader in lateral view. In anterior view the axis has a thickened, triangular neural spine. Below the neural spine, at the lateral margins of the neural arch, the anteroventrally directed prezyga-pophysis is relatively short in comparison with those of the other cervicals. The rounded axial centrum is similar to that of the atlas, and lateral to the centrum a transverse
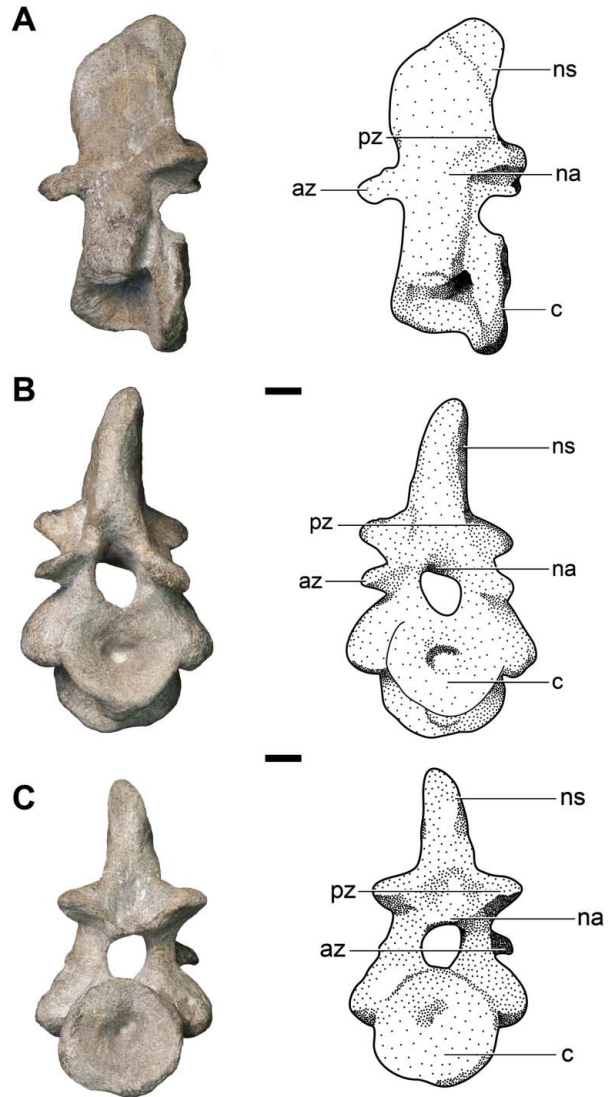

Figure 17. Photographs and drawings of the axis of *Anteosaurus magnificus* BP/1/7074; **A,** lateral view; **B,** anterior view; and **C,** posterior view. Abbreviations: az, anterior zygapophysis; c, centrum; na, neural arch; ns, neural spine; pz, posterior zygapophysis. Scale bars = 10 mm.
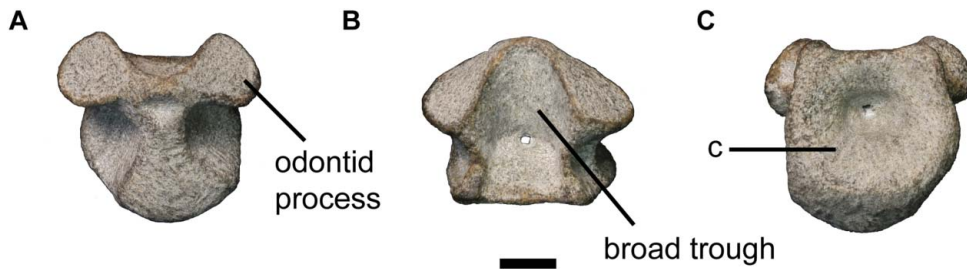

Figure 16. Atlas centrum of *Anteosaurus magnificus* BP/1/7074; **A,** anterior view; **B,** dorsal view; and **C,** posterior view. Abbreviation: c, centrum. Scale bar = 10 mm.
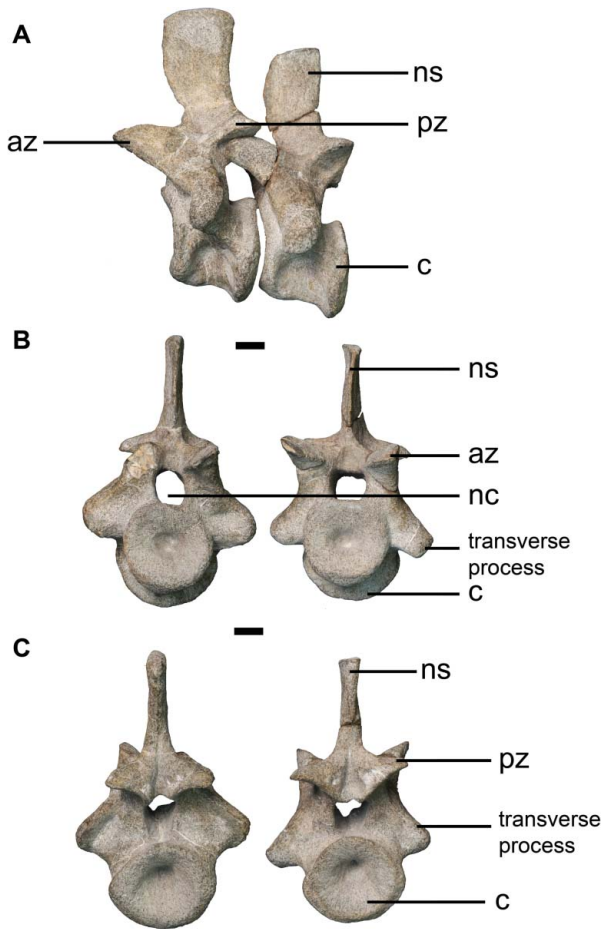
Figure 18. Third and fourth cervical vertebrae of *Anteosaurus magnificus* BP/1/7074; **A,** lateral view; **B,** anterior view; and **C,** posterior view. Abbreviations: az, anterior zygapophysis; c, centrum; na, neural arch; nc, neural canal; ns, neural spine; pz, posterior zygapophysis. Scale bars = 10 mm.

process is present which extends farther ventrally than those of the post-axial vertebrae. In posterior view, the centrum is round and deeply amphicoelous. Ventral to the neural spine, the postzygapophysis has ventrally positioned facets lateral to the anterior margin of the neural arch. Between the postzygapophyses a deep diamond-shaped hollow is present.

The third and fourth cervical vertebrae are similar in size and shape (Fig. 18). In anterior view, the centrum is round and deeply amphicoelous. The prezygapophyses are longer than those of the axis, and have dorsomedially facing facets. The axis and third and fourth cervical vertebrae each have a small fossa on the lateral surface of the neural arch.

Discussion

The fact that BP/1/7074, which is a relatively small specimen, has a concave alveolar margin of the precanine

region, concave dorsal snout profile, posterolateral cant of the posteriormost upper postcanines and anteroventrally rotated suspensorium and was found in the same stratigraphic horizon as larger specimens of *Anteosaurus magnificus* suggests that it is a juvenile of this species. The juvenile status of the specimen is demonstrated by the fact that many of the bones of the skull roof have come apart at the sutures, and the orbits are proportionally large when compared to the size of the temporal opening. In addition, pachyostosis of the frontal bone of BP/1/7074 is poorly developed. *Anteosaurus* is represented by approximately 30 specimens of differing size from the South African Karoo (Kammerer 2011).

Comparison of BP/1/7074 with the small South African anteosaurid *Australosyodon* (basal skull length 240 mm) shows important differences, such as the snout of *Australosyodon* being much narrower and almost at the same plane as the rest of the skull roof. *Australosyodon* has an incipient heel on the lingual side of the lower incisors, canines that are laterally flattened and have a sharp keel on their posteromedial edge, and two distinct rows of teeth on the palatine boss, all features which are not present in BP/1/7074. In addition, the vomers of *Australosyodon* curve medially and ventrally to a greater degree than those of BP/1/7074. The maxilla-premaxillary suture is immediately posterior to the paracanine fossa in *Australosyodon*, whereas in BP/1/7074 it crosses the aforementioned fossa. These differences suggest that BP/1/7074 cannot be referred to *Australosyodon*.

Apart from the snout fragment of the specimen originally described as the holotype of *Micranteosaurus parvus* (Boonstra 1954b), which is now considered to be a small individual of *Anteosaurus magnificus* (Boonstra 1969; Kammerer 2011), the length of the *Anteosaurus* skull was known to range between 480 and 805 mm (Boonstra 1954a, p. 144). The newly discovered skull of BP/1/7074, with a length of 280 mm, is therefore the smallest complete skull of *Anteosaurus magnificus* to date and is roughly one-third of the adult size. As this specimen is relatively well preserved, it provides a good opportunity to analyse ontogenetic changes that occur in this taxon.

Despite the constraints of a small sample size (*n* between 6 and 10), and because most *Anteosaurus* skulls are incompletely preserved, our analysis demonstrates allometric growth for characters that exhibit extreme differences between the smallest and largest specimens of the sample (Fig. 19). The allometry coefficient suggests that fast growth occurred in the temporal region, which is likely related to a key therapsid feature: the mandibular adductor musculature (Table 1). Associated with the growth of the temporal region, the postorbital bar and suborbital bar (height of jugal below the orbit) are strongly positive (Table 1). Finally, positive allometry occurs at the anterior tip of the snout,
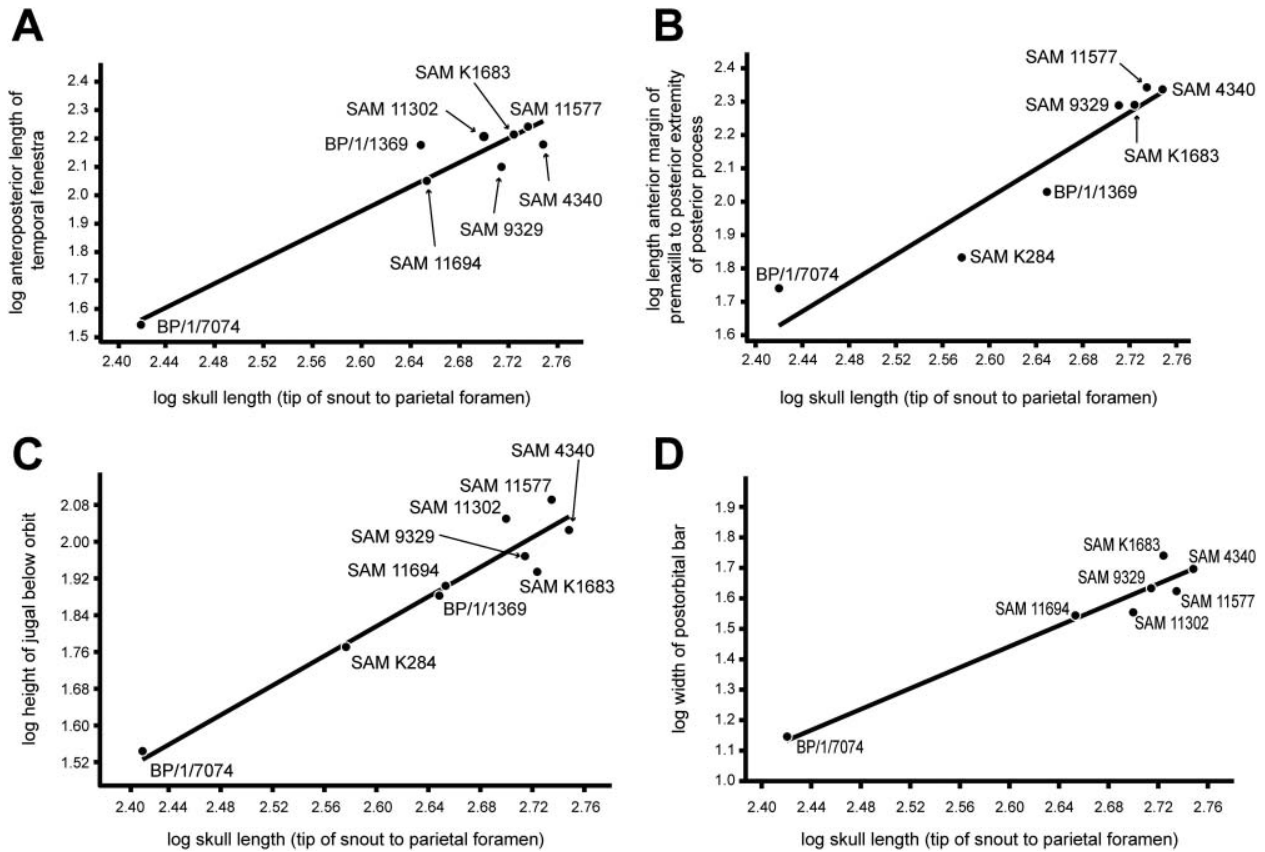
Figure 19. Results of the allometric analysis indicating regression of length of the skull (tip of snout to parietal foramen) (log Variable 4) on **A,** anteroposterior length of the temporal fenestra (log Variable 7) $b_1 = 2.44$; **B,** length of the anterior margin of premaxilla to the posterior extremity of posterior process (log Variable 13) $b_1 = 2.13$; **C,** height of the jugal below the orbit (log Variable 21) $b_1 = 1.61$; and **D,** width of postorbital bar (log Variable 22) $b_1 = 1.71$.

but the length of the entire snout grows isometrically (see variable 5 in Table 1).

Additional trends, assessed qualitatively, can be added to the quantitative growth model of *Anteosaurus*. The orbits are proportionally smaller in larger specimens of *Anteosaurus*, a condition that fits in the expected negative allometry of cranial structures related to the brain and sense organs in vertebrates (Emerson & Bramble 1993), and in this case is probably associated with the strong positive allometry of the postorbital and suborbital bars. Larger *Anteosaurus* specimens show an increase in the angle between the nasal and the frontal, as the skull roof slopes sharply dorsally and the height of the skull increases posteriorly from the level of the frontal bones, reaching its highest level at the parietal foramen.

In addition to the positive allometry of the length of the temporal fenestra, it can be noted that the fenestra appears proportionally wider in adults, indicating fast growth in both length and width. These changes result in the occiput being positioned relatively farther behind the orbits in larger adult specimens. On the skull roof, the pineal boss increases in height and pachyostosis occurs in larger

specimens. Although BP/1/7074 does have a slight pineal boss, the swelling of this boss is much less than that of larger specimens.

The lateral edges of the vomers curve ventromedially in BP/1/7074, whereas in larger specimens they extend ventrally. The juvenile has a tooth on the pterygoid boss (Fig. 10), whereas there are no teeth on this structure in the adults (Boonstra 1954a; Kammerer 2011, p. 301, character 13).

There are other observed differences between juvenile and adult *A. magnificus* that are likely related to ontogeny. The frontal slopes downward towards the rostrum more steeply with size, and also in larger specimens the side of the skull projects farther laterally posterior to the orbits, and the parietal foramen is raised higher above the dorsal skull. In contrast to the situation on the skull roof, in the palate there is only a gradual increase in relative size, and there are not many changes in the palatal bones, other than the loss of palatal dentition. Thus, the relatively greater ontogenetic modifications on the skull roof compared to those of the palate have resulted in the dorsal side of the occiput being located farther posteriorly than

the ventral side in adults. The most remarkable difference is the placement of the lateral process of the pterygoids; they are located much more anteriorly in adults.

Specimen BP/1/7074 has nine postcanine tooth positions in each maxilla, the largest number in *A. magnificus*. Variation in postcanine number previously reported for this taxon was between five and eight (Boonstra 1954a). However, because of the relatively small sample of specimens, it is not possible to establish an ontogenetic trend as the individual variation in tooth number in presumed adults is between five and seven and does not correlate with the size of the individual (Table 1).

Comparative ontogeny of Anteosauria

The cranial ontogeny of the Chinese anteosaurid *Sinophoneus yumenesis* was recently studied by Liu (2013), based on skull size varying in length from 113 mm to 315 mm. The adult of this species is slightly larger than that of the juvenile *Anteosaurus magnificus* described here. In addition, ontogenetic skull variations are also represented in *Titanophoneus potens*, with subadults having a skull length of ~410 mm and adults of 500 mm (Orlov 1958; Kammerer 2011). Trends shared between these species and *A. magnificus* include a greater degree of pachyostosis of the skull in larger specimens (Liu 2013; Kammerer 2011, figs 6B, 7B). Another ontogenetic feature described in *Sinophoneus* is the degree of development of the midline dorsal ridge of the skull, which is faint in juveniles and conspicuous in adults. Ontogenetic modification of the skull roof of *A. magnificus* includes greater pachyostosis, as adults of the species develop a huge frontal bone that completely changes the dorsal profile of the skull (compare Fig. 20A and 20E). Another similarity in the ontogeny of *Sinophoneus* and *Anteosaurus* is the positive allometry of the temporal region (Liu 2013, p. 1406). However, the direction of the expansion of the fenestra in the two species differs as it is mainly dorsally in *Sinophoneus* and posteriorly in *Anteosaurus*. Enlargement of the temporal fenestra is also manifested in *Titanophoneus potens* in which the adult has a longer and laterally wider fenestra (Orlov 1958; Kammerer 2011). The expansion of this fenestra is an expected ontogenetic trend likely connected with the enlargement of the adductor mandibulae externus muscle in adults (Barghusen 1973, 1975).

Another trend reported for *Sinophoneus* is the increase of palatal width as indicated by strong positive allometry of the width of the transverse processes of the pterygoid (Liu 2013). Although we do not have any variables measured on the palate because of the poor preservation of our sample, qualitative comparison of the palatal view of BP/1/7074 with those of larger specimens of *Anteosaurus* shows the palate to be comparatively wider and slightly shorter in adults. The latter condition is inferred from the relatively posterior position of the lateral processes of the
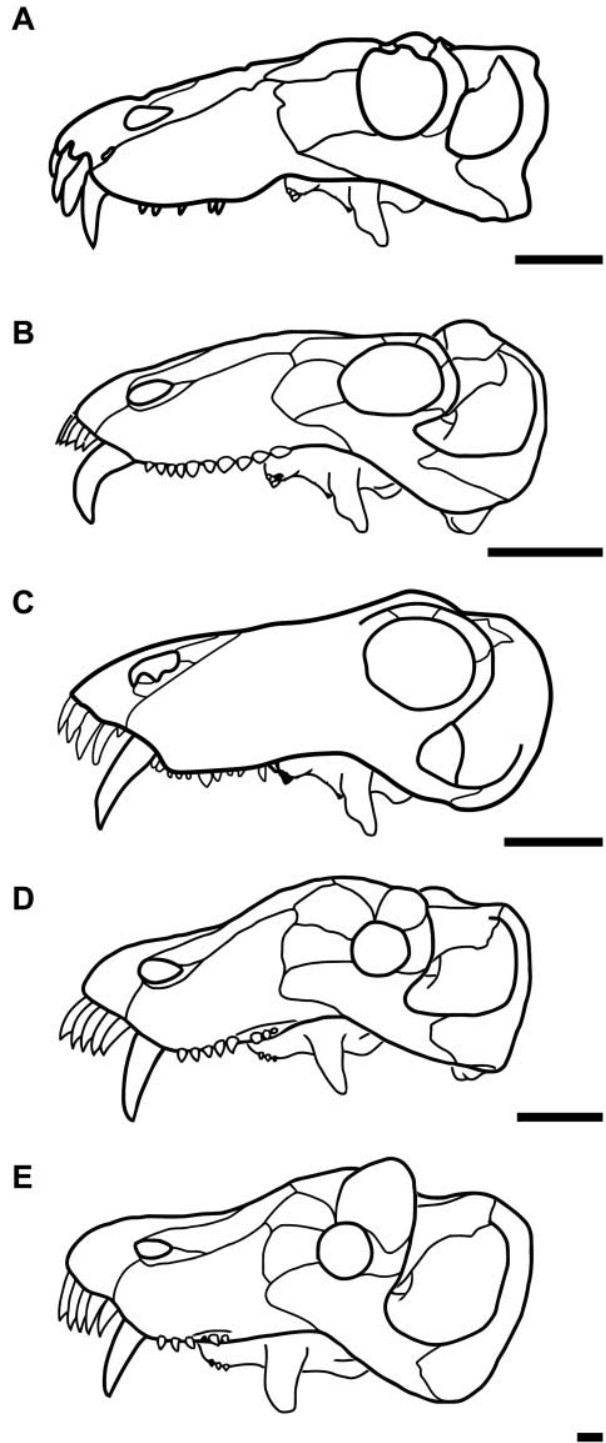

Figure 20. Skulls and skull lengths of anteosaurids. **A,** juvenile *Anteosaurus magnificus* (BP/1/7074); **B,** *Syodon biarmicum*; **C,** *Australosyodon nyaphuli*; **D,** *Titanophoneus potens*; and **E,** an adult *Anteosaurus magnificus* in left lateral view. Scale bars = 50 mm. (B, D and E redrawn after Kammerer 2011, p. 292).
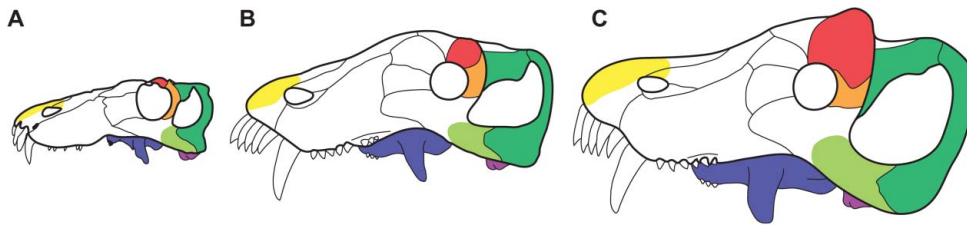
Figure 21. Ontogenetic changes in the skull of *Anteosaurus*; **A,** juvenile; **B,** intermediate sized; **C,** adult sized. (C redrawn after Kammerer 2011, p. 292).

pterygoid in BP/1/7074. Similar ontogenetic variation in the placement of this process is observed in *Titanophoneus* (Orlov 1958), but this trend is absent in the ontogeny of *Sinophoneus* (F. Abdala pers. obs. 2016). Another trend of *Anteosaurus*, which is present in both *Titanophoneus* (Kammerer 2011) and *Sinophoneus* (Liu 2013), is the decrease in palatal tooth number.

In general, from comparison of the skull morphology of BP/1/7074 with that of other adult anterosaurid specimens (Fig. 20), it is clear that the juvenile cranial morphology of *Anteosaurus* is reminiscent of the adult morphology of the Russian syodontine *Syodon biarmicum*. This overall similarity is most likely related to the size of the specimens and its correlation with a lesser degree of pachyostosis, which plays an important role in modifying the skull roof of adults. This is perhaps a component of sexual dimorphism in *Anteosaurus* (Barghusen 1975). The juvenile *Anteosaurus* (BP/1/7074) has a skull length of 280 mm, which is slightly larger than the adult skull length of 218 mm of *Syodon* (PIN 157/2). The marked degree of skull roof pachyostosis in adult *Anteosaurus* specimens that reach a skull length of 800 mm is only incipiently manifested in *Syodon* and the juvenile *Anteosaurus* (differences in the degree of skull roof pachyostosis is also manifested in subadult and adult specimens of *Titanophoneus*). Linked with the degree of skull roof pachyostosis is the size of the orbit, which is proportionally larger in juvenile *Anteosaurus* and adult *Syodon* than in adult *Anteosaurus*. A trait such as the posterior position of the transverse process of the pterygoid, directly connected not with pachyostosis but with the development of the palate, also shows a clear similarity between the juvenile *Anteosaurus* and the adult *Syodon* (Fig. 20A, B).

Conclusions

Adult characters of *Anteosaurus* are massively pachyostosed postfrontals as well as a massive frontal boss, concave alveolar margin of the precanine region, and concave dorsal snout profile.

The ontogenetic series of *Anteosaurus magnificus* is represented by skull lengths varying from 280 to 805 mm. The most important morphological modifications of the

skull are the development of pachyostosis, the positive allometries of the temporal opening, and the postorbital and suborbital bars, which become increasingly robust in adults (Fig. 21). The anterior portion of the snout also grew relatively faster. Adults show proportionally smaller orbits and an increase in the angle between the nasal and the frontal. On the skull roof, the pineal boss increases in height and there is a greater degree of pachyostosis around it. Some of these cranial changes (i.e. pachyostosis and positive allometry of the temporal opening) are also ontogenetic trends described for the Chinese anteosaurid *Sinophoneus yumenesis*, and have been observed in the Russian *Titanophoneus potens*.

The cranial morphology of juvenile *Anteosaurus* appears broadly similar to that of the Russian *Syodon*. Evidence of an ontogenetic correlation between the degree of skull roof pachyostosis and the size of the animal has been shown in all anteosaurids. It is interesting to point out that ontogenetic shortening of the palate in *Titanophoneus* and *Anteosaurus* (recognized by the more anterior placement of the lateral process of the pterygoid in adults) is not manifested in the ontogeny of *Sinophoneus*.

whose critiques and suggestions have greatly enhanced this work.

Supplemental material

Supplemental material for this article can be accessed at: http://dx.doi.org/10.1080/14772019.2016.1276106.

ORCID

Ashley Kruger http://orcid.org/0000-0003-1196-8693

References

Abdala, F. & **Giannini, N. P.** 2000. Gomphodont cynodonts of the Chañares Formation: the analysis of an ontogenetic sequence. *Journal of Vertebrate Paleontology*, **20**, 501–506.

Barghusen, H. R. 1973. The adductor jaw musculature of *Dimetrodon* (Reptilia, Pelycosauria). *Journal of Paleontology*, **47**, 823–834.

Barghusen, H. R. 1975. A review of fighting adaptations in Dinocephalia (Reptilia, Therapsida). *Paleobiology*, **1**, 295–311.

Boonstra, L. D. 1954a. The cranial structure of the titanosuchian: *Anteosaurus*. *Annals of the South African Museum*, **42**, 108–148.

Boonstra, L. D. 1954b. The smallest titanosuchid yet recovered from the Karoo. *Annals of the South African Museum*, **42**, 149–156.

Boonstra, L. D. 1954c. *Paranteosaurus*, gen. nov.: a Titanosuchian reptile. *Annals of the South African Museum*, **42**, 157–159.

Boonstra, L. D. 1963. Diversity within the South African Dinocephalia. *South African Journal of Science*, **59**, 196–206.

Boonstra, L. D. 1969. The fauna of the *Tapinocephalus* Zone (Beaufort beds of the Karoo). *Annals of the South African Museum*, **56**, 1–73.

Boonstra, L. D. 1971. The early therapsids. *Annals of the South African Museum*, **59**, 17–46.

Boos, A. D. S., **Kammerer, C. F.**, **Schultz, C. L.** & **Paes Neto**, V. **D.** 2015. A tapinocephalid dinocephalian (Synapsida, Therapsida) from the Rio do Rasto Formation (Paraná Basin, Brazil): taxonomic, ontogenetic and biostratigraphic considerations. *Journal of South American Earth Sciences*, **63**, 375–384.

Broom, R. 1905. On the use of the term Anomodontia. *Records of the Albany Museum*, **1**, 266–269.

Cheng, Z. W. & **Ji, S.** 1996. First record of a primitive anteosaurid dinocephalian from the Upper Permian of Gansu, China. *Vertebrata PalAsiatica*, **34**, 123–134.

Cheng, Z. & **Li, J.** 1997. A new genus of primitive dinocephalian: the third report on Late Permian Dashankou lower tetrapod fauna. *Vertebrate PalAsiatica*, **35**, 35–43.

Cisneros, J. C., **Abdala, F.**, **Atayman-Guven, S.**, **Rubidge, B. S.**, **Celal, Sengor**, **A. M.** & **Shultz, C. L.** 2012. Carnivorous dinocephalian from the middle Permian of Brazil and tetrapod dispersal in Pangaea. *Proceedings of the National Academy of Sciences, USA*, **109**, 1584–1588.

Day, M. O. 2013. *Middle Permian continental biodiversity change as reflected in the Beaufort Group of South Africa: a bio- and lithostratigraphic review of the Eodicynodon, Tapinocephalus*

and Pristerognathus Assemblage Zones. Unpublished PhD thesis, University of the Witwatersrand, 387 pp.

Day, M. O., **Güven, S.**, **Abdala, F.**, **Jirah, S.**, **Rubidge, B. S.** & **Almond, J.** 2015. Youngest dinocephalian fossils extend the *Tapinocephalus* Zone, Karoo Basin, South Africa. *South African Journal of Science*, **111**, 1–5.

Efremov, I. A. 1954. [The terrestrial vertebrate fauna from the Permian copper sandstones of the western Fore-Urals]. *Trudy Paleontologicheskogo Instituta, Akademiya Nauk SSSR*, **54**, 1–416. [In Russian.]

Emerson, S. B. & **Bramble, D. M.** 1993. Scaling, allometry and skull design. Pp. 384–416 in J. Hanken & B. K. Hall (eds) *The skull*. University of Chicago Press, Chicago.

Hammer, ∅., **Harper, D. A. T.** & **Ryan, P. D.** 2001. PAST: paleontological statistics software package for education and data analysis. *Palaeontologia Electronica*, **4**, 9.

Ivachnenko, M. F. 1995. Primitive Late Permian dinocephalian-titanosuchids of Eastern Europe. *Paleontological Journal*, **29**, 120–129.

Ivachnenko, M. F. 2000. *Estemmenosuchus* and primitive theriodonts from the Late Permian. *Paleontological Journal*, **34**, 189–197.

Jirah, S. & **Rubidge, B. S.** 2014. Refined stratigraphy of the middle Permian Abrahamskraal Formation (Beaufort Group) in the southern Karoo Basin. *Journal of African Earth Sciences*, **100**, 121–135.

Kammerer, C. F. 2011. Systematics of the Anteosauria (Therapsida: Dinocephalia). *Journal of Systematic Palaeontology*, **9**, 261–304.

Kemp, T. S. 2005. *The origin and evolution of mammals*. Oxford University Press, Oxford, 342 pp.

Lepper, J., **Raath, M. A.** & **Rubidge, B. S.** 2000. A diverse dinocephalian fauna from Zimbabwe. *South African Journal of Science*, **96**, 403–405.

Li, J. & **Cheng, Z.** 1995. A new Late Permian vertebrate fauna from the Dashankou, Gansu with comments on Permian and Triassic vertebrate assemblage zones of China. Pp. 33–37 in A. I. Sun & Y. Q. Wang (eds) *Short papers of sixth symposium on Mesozoic terrestrial ecosystems and biota*. China Ocean Press, Beijing.

Li, J., **Rubidge, B. S.** & **Cheng, Z.** 1996. A primitive anteosaurid dinocephalian from China – implications for the distribution of earliest therapsid faunas. *South African Journal of Science*, **92**, 252–253.

Liu, J. 2013. Osteology, ontogeny and phylogenetic position of *Sinophoneus yumenensis* (Therapsida, Dinocephalia) from the middle Permian Dashankou Fauna of China. *Journal of Vertebrate Paleontology*, **33**, 1394–1407.

Nicolas, M. & **Rubidge, B. S.** 2010. Changes in Permo–Triassic terrestrial tetrapod ecological representation in the Beaufort Group (Karoo Supergroup) of South Africa. *Lethaia*, **43**, 45–59.

Orlov, J. A. 1958. [Predatory dinocephalians from the Isheevo Fauna (titanosuchians)]. *Trudy Paleontologicheskogo Instituta, Akademiya Nauk SSSR*, **72**, 1–114. [In Russian.]

Osborn, H. F. 1903. On the primary division of the Reptilia into two sub-classes, Synapsida and Diapsida. *Science*, **17**, 275–276.

Rubidge, B. S. 1991. A new primitive dinocephalian mammal-like reptile from the Permian of southern Africa. *Palaeontology*, **34**, 547–559.

Rubidge, B. S. 1994. *Australosyodon*, the first primitive anteosaurid dinocephalian from the Upper Permian of Gondwana. *Palaeontology*, **37**, 579–594.

Rubidge, B. S. & **van den Heever, J. A.** 1997. Morphology and systematic position of the dinocephalian *Styracocephalus platyrhychus*. *Lethaia*, **30**, 157–168.

Seeley, H. G. 1894. Researches on the structure, organisation, and classification of the fossil Reptilia. Part VIII. Further evidence of *Deuterosaurus and Rhopalodon* from the Permian rocks of Russia. *Philosophical Transactions of the Royal Society of London*, **185**, 663–717.

Sidor, C. A. 2003. The naris and palate of *Lycaenodon longiceps* (Therapsida: Biarmosuchia), by comments on their early evolution in the Therapsida. *Journal of Paleontology*, **77**, 977–984.

Sidor, C. A., **Angielczyk, K. D.**, **Smith, R. M.**, **Goulding, A. K.**, **Nesbitt, S. J.**, **Peecook, B. R.** & **Tolan, S.** 2014. Tapinocephalids (Therapsida, Dinocephalia) from the Permian Madumabisa Mudstone Formation (Lower Karoo, Mid-Zambezi Basin) of southern Zambia. *Journal of Vertebrate Paleontology*, **34**, 980–986.

Simon, R. V., **Sidor, C. A.**, **Angielczyk, K. D.** & **Smith, R. M. H.** 2010. First record of a Tapinocephalid (Therapsida: Dinocephalia) from the Ruhuhu Formation (Songea Group) of Southern Tanzania. *Journal of Vertebrate Paleontology*, **30**, 1289–1293.

Smith, R., **Rubidge, B. S.** & **van der Walt, M.** 2011. Therapsid biodiversity patterns and paleoenvironments of the Karoo Basin, South Africa. Pp. 30–62 in A. Chinsamy-Turan (ed.) *Forerunners of mammals: radiation, histology, biology*. Indiana University Press, Bloomington.

Tchudinov, P. K. 1968. A new Dinocephalion from the Cisuralian Region (Reptilia, Therapsida; Upper Permian). *Postilla*, **121**, 1–20.

Watson, D. M. S. 1921. The bases of classification of the Theriodontia. *Proceedings of the Zoological Society of London*, **1921**, 35–98.